J|A|C|S ARTICLES

Published on Web 04/28/2010

Accessing Ultrashort Reaction Times in Particle Formation with SAXS Experiments: ZnS Precipitation on the Microsecond Time Scale

Wolfgang Schmidt,*,† Patrick Bussian,†,‡ Mika Lindén,§ Heinz Amenitsch,|| Patrik Agren,†,⊥ Michael Tiemann,§,# and Ferdi Schüth†

Max-Planck-Institut für Kohlenforschung, Kaiser-Wilhelm-Platz 1, D-45470 Mülheim an der Ruhr, Germany, Center for Functional Materials, Department of Physical Chemistry, Åbo Akademi University, Porthansgatan 3-5, FIN-20500 Turku, Finland, Institute of Biophysics and Nanosystems Research, Austrian Academy of Sciences, Schmiedlstr. 6, A-8042 Graz, Austria

Received February 23, 2010; E-mail: schmidt@kofo.mpg.de

Abstract: Precipitation of zinc sulfide particles is a very rapid process, and monitoring of the particle growth is experimentally very demanding. Applying a liquid jet flow cell, we were able to follow zinc sulfide particle formation on time scales down to 10^{-5} s. The flow cell was designed in such a way that data acquisition on the microsecond time scale was possible under steady-state conditions along a liquid jet (tubular reactor concept), allowing SAXS data accumulation over a time scale of minutes. We were able to monitor the growth of zinc sulfide particles and found experimental evidence for very rapid particle aggregation processes within the liquid jet. Under the experimental conditions the particle growth is controlled by mass transfer: i.e., the diffusion of the hydrogen sulfide into the liquid jet.

Introduction

Despite the fact that the formation of particles has been studied for many decades, it is still a very elusive process. While textbook knowledge assumes nucleation and growth mechanisms for the formation of particles from solution in precipitation reactions, in many cases it seems clear that it is rather a sequence of complex reaction steps. The difficulties in the elucidation of particle formation reactions arise from the fact that there are almost no suitable analytical techniques to monitor such processes, especially not for the analysis of very fast reactions, such as the precipitation of sulfides of the elements of groups 7−12. Spectroscopic methods allow monitoring processes in the submillisecond range but provide only local information. Methods providing long-range information usually require extended data acquisition time and are thus hardly applicable for monitoring particle formation. Transition-metal sulfides, which are important materials for optoelectronic applications, are usually obtained by precipitation in aqueous solution, a very rapid process on a time scale which is typically not accessible by conventional characterization methods. As a consequence, the early stages of particle formation and growth of transition-metal sulfides are still elusive. In 1999 we had introduced a continuous-flow reactor to study the formation of ordered mesoporous materials on the time scale of minutes.[1−4] However, such flow reactors have substantial limitations. They do not allow assessment of time scales below milliseconds, because sufficient mixing of the reagents cannot be achieved on shorter time scales. In addition, they have walls creating laminar flow profiles leading to axial dispersion and, thus, less well-defined residence times as would be possible for a plug-flow system. Moreover, they are a source for incrustation (fouling) and heterogeneous nucleation. Nowadays, fast reactions and mixing can be performed in microfluidic systems.[5] However, fouling on the walls and clogging of microfluidic channels remains a serious problem. Another approach to study the kinetics of fast precipitation reactions in situ is the combination of spectroscopic techniques with the stopped-flow method. As we have shown earlier, the size evolution of ZnS particles can be studied in the millisecond time regime by using the size-dependent UV absorption signature of nanosized ZnS particles as a spectroscopic probe. The outcome of our studies was the growth of primary particles with sizes between 1 and 1.5 nm with strong ripening phenomena.[6−8] MD and DFT calculations suggest that

† Max-Planck-Institut für Kohlenforschung.
‡ Present address: SASOL Germany GmbH, Anckelmannsplatz 1, D-20537 Hamburg, Germany.
§ Åbo Akademi.
|| Institute of Biophysics and Nanosystems Research.
⊥ Present address: Vaisala Oyj, P.O. Box 26, FIN-00421 Helsinki, Finland.
Present address: Department of Chemistry, University of Paderborn, Warburger Str. 100, 33098 Paderborn, Germany.

(1) Lindén, M.; Schunk, S. A.; Schüth, F. *Angew. Chem.* **1998**, *110*, 871.
(2) Lindén, M.; Schunk, S. A.; F.Schüth., F. *Stud. Surf. Sci. Catal.* **1998**, *117*, 45.
(3) Linden, M.; Blanchard, J.; Schacht, S.; Schunk, S. A.; Schüth, F. *Chem. Mater.* **1999**, *11*, 2002.
(4) Schüth, F.; Bussian, P.; Ågren, P.; Schunk, S. A.; Lindén, M. *Solid State Sci.* **2001**, *3*, 801.
(5) Marmiroli, B.; Grenci, G.; Cacho-Nerin, F.; Sartori, B.; Ferrari, E.; Laggner, P.; Businarob, L.; Amenitsch, H. *Lab Chip* **2009**, *9*, 2063.
(6) Tiemann, M.; Weiβ, Ö.; Hartikainen, J.; Marlow, F.; Lindén, M. *ChemPhysChem* **2005**, *6*, 2113.
(7) Tiemann, M.; Marlow, F.; Brieler, F.; Lindén, M. *J. Phys. Chem. B* **2006**, *110*, 23142.
(8) Tiemann, M.; Marlow, F.; Hartikainen, J.; Weiβ, Ö.; Lindén, M. *J. Phys. Chem. C* **2008**, *112*, 1463.

10.1021/ja101519z

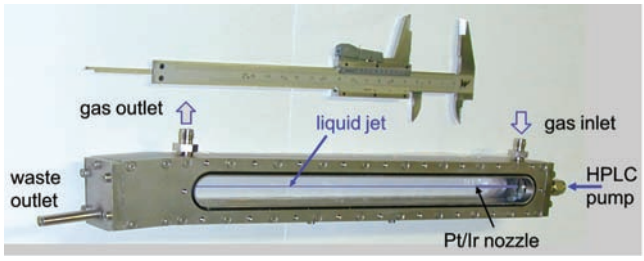

Figure 1. Jet flow cell and experimental setup. The X-ray beam passes through the liquid jet perpendicular to the jet direction.

in the early stages of ZnS particle formation neither the sphalerite nor the wurtzite structures are formed but initially rather sulfur-rich ZnS_x clusters of defined sizes.[9−12] With increasing sizes, successively small bubble clusters of composition $(ZnS)_n$ with rather stable configurations form, followed by bubble clusters consisting of multiple bubbles if n is increasing.[13] At cluster sizes of more than about 2−3 nm Catlow and coworkers predicted clusters with $n = 256$ and 512 having crystalline interiors,[14] the crystal structures of which were neither sphalerite nor wurtzite but were related to the BCTT zeolite structure. Clusters with both sphalerite and wurtzite structures would be less stable, with a sphalerite cluster being the least stable species.[12] However, up to now, no experimental evidence has been found for the presence of clusters with the proposed structure. Nevertheless, theoretical calculations as well as stopped-flow experiments strongly suggest a ripening process during the formation of the smaller ZnS particles, referred to here as primary particles. Aggregation and agglomeration of the primary particles to form larger secondary particles have been not accounted for in the previous investigations. However, the probability that such processes occur is very high.

In the following, we will show data which demonstrate that zinc sulfide formation proceeds on an extremely short time scale (10^{-5} s) with virtually no indication of an induction time. To overcome the limitations of conventional liquid flow reactors with respect to clogging of channels and fouling on reactor walls or windows, we developed a liquid jet reactor in which the second reaction component is fed into the liquid jet from the gas phase.

Experimental Section

In situ SAXS data have been measured on the liquid jet in the novel type of continuous reactor. The reaction cell is made of a stainless steel body equipped with two polymer windows. Into this reactor a single-component Zn^{2+} precursor solution is injected through a pinhole (nozzle) into a flowing H_2S gas atmosphere. The jet passes the cell perpendicular to the X-ray beam and parallel to the two polymer windows, as illustrated in Figure 1 (see also the Supporting Information). The liquid jet cell has been integrated into a SAXS setup which provides an X-ray beam with a diameter of 0.5 mm. A typical jet velocity was 47 m s^{-1}, corresponding to a reaction time of 10.6 μs if the first data point is taken at a distance of 0.5 mm (center of the X-ray beam) from the nozzle. In order to realize longer reaction times, either the flow was reduced or data points were collected further away from the nozzle.

For the experiments a jet of aqueous zinc chloride solution (1, 0.1, or 0.01 mol L^{-1}) was injected into an atmosphere containing hydrogen sulfide gas (H_2S) admixed with nitrogen in a H_2S/N_2 ratio of 1/3 at a total flow of 40 mL min^{-1}. Experiments with higher concentrations of hydrogen sulfide have also been performed by passing pure hydrogen sulfide through the flow jet cell at a flow rate of 20 mL min^{-1}. When the liquid jet is injected into the gas atmosphere, hydrogen sulfide diffuses into the aqueous zinc chloride solution and dissociates into protons and hydrosulfide (SH^-) anions (under near-neutral pH conditions), which then react with cationic zinc species (Zn^{2+}, $ZnOH^+$)[7,15] to form zinc sulfide, accompanied by further deprotonation. At every point along the longitudinal axis of the liquid jet the proceeding reaction can be monitored under steady-state conditions (tubular reactor concept), allowing data acquisition over several minutes. Typical data acquisition times were 300 s. Stepwise data collection at different positions along the longitudinal axis of the jet provided time-resolved information on particle formation. The salt solution was injected with a HPLC pump at constant pumping rates of 3.5−5.5 mL min^{-1}. Using 50 μm nozzles, the liquid jet was injected at a velocity of 47 m s^{-1} corresponding to 21.3 μs per millimeter of jet length. Particles formed after longer residence times were investigated using 80 μm nozzles applying jet velocities of 11.5−18.3 m s^{-1}. At maximum jet velocity, a laminar gas flow can be expected for the first 35 mm of the liquid jet (see the Supporting Information). Turbulent gas flow at distances further away from the nozzle resulted in occasional spraying which, in turn, caused droplets on the windows of the jet cell. Particle formation in such droplets easily could adulterate the scattering experiments. Thus, the cell windows were carefully checked after each measurement to ensure reliable data. Background measurements have been performed on liquid jets of the respective $ZnCl_2$ solutions under a pure nitrogen atmosphere.

The measurements were conducted at the SAXS beamline of the Austrian Academy of Sciences at the Elettra synchrotron radiation source in Trieste, Italy,[16] utilizing a linear position sensitive Gabriel detector. The SAXS camera was set to a length of 1.5 m and to a photon energy of 8 keV. In order to prevent contamination of the air in the experiment hutch with the poisonous hydrogen sulfide, the whole setup was installed in a gastight housing with polymer windows, which was attached to the gas exhaust system of the beamline (see the Supporting Information). The observed scattering curves have been corrected for measured background data and evaluated using the Guinier approximation for $qR \ll 1$ and/or the Porod approximation for $qR \gg 1$. For some data sets, local fits of the scattering curve were obscured by strong background and low signal-to-noise ratio. In those cases, a unified equation, as introduced by Beaucage,[17,18] has been used to fit scattering curves over the full q range, allowing simultaneous evaluation of radii of gyration and Porod constants.

Results and Discussion

From our experimental data, one cannot deduce whether the formed particles in fact possess crystalline structures of any of the aforementioned ZnS or ZnS_x, of $(ZnS)_n$ phases. For simplicity, the particles will be denoted as ZnS, irrespective of their real structures. Figure 2 shows typical examples of scattering curves as obtained at very short reaction times. From the scattering data in the Guinier range as shown in Figure 2a, radii of gyration and the radii of the respective particles present

(9) Matxain, J. M.; Fowler, J. E.; Ugalde, J. M. *Phys. Rev. A* **2000**, *61*, 053201–053208.
(10) Hamad, S.; Catlow, C. R. A.; Spanó, E.; Matxain, J. M.; Ugalde, J. M. *J. Phys. Chem. B* **2005**, *109*, 2703–2709.
(11) Hamad, S.; Cristol, S.; Catlow, C. R. A. *J. Am. Chem. Soc.* **2005**, *127*, 2580–2590.
(12) Catlow, C. R. A.; Bromley, S. T.; Hamad, S.; Mora-Fonz, M.; Sokol, A. A.; Woodley, S. M. *Phys. Chem. Chem. Phys.* **2010**, *12*, 786–811.
(13) Spanó, E.; Hamad, S.; Catlow, C. R. A. *Chem. Commun.* **2004**, 864–865.
(14) Hamad, S.; Catlow, C. R. A. *J. Cryst. Growth* **2006**, *294*, 2–8.
(15) Hayashi, K.; Sugaki, A.; Kitakaze, A. *Geochim. Cosmochim. Acta* **1990**, *54*, 715.
(16) Amenitsch, H.; Rappolt, M.; Kriechbaum, M.; Mio, H.; Laggner, P.; Bernstorff, S. *J. Synchrotron Radiat.* **1998**, *5*, 506.
(17) Beaucage, G. *J. Appl. Crystallogr.* **1995**, *28*, 717.
(18) Beaucage, G. *J. Appl. Crystallogr.* **1996**, *29*, 134.

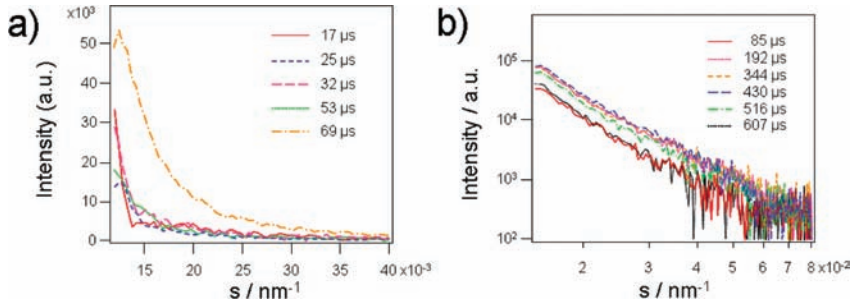

Figure 2. Typical SAXS data of ZnS particles as observed from liquid jets of 1 mol L^{-1} $ZnCl_2$ solution under a 10/30 H_2S/N_2 atmosphere: (a) plots at residence times shorter than 70 μs; (b) Porod plots of data measured for longer residence times.

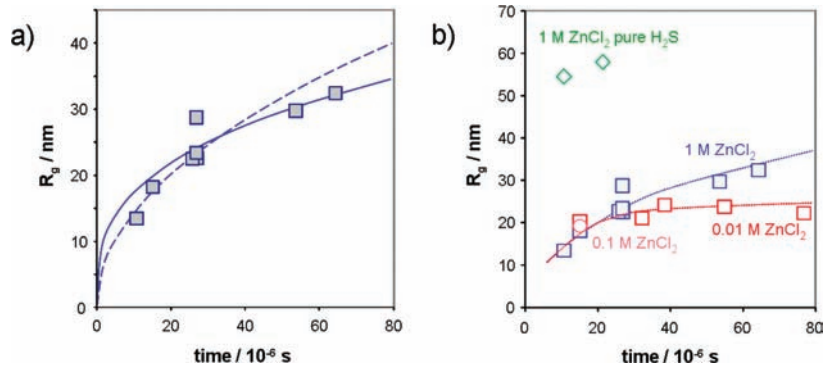

Figure 3. (a) Radii of gyration, R_g, of ZnS particles as observed after ultrashort reaction times using 1 mol L^{-1} $ZnCl_2$ solution under a 10/30 H_2S/N_2 gas atmosphere (■). The dashed line shows the best fit assuming $t^{1/2}$ dependence (diffusion-controlled process, $V(t) = \text{const} \times t^{1/2}$) and the solid line $t^{1/3}$ dependence (reaction-controlled process, $V(t) = \text{const} \times t^{1/3}$) of the ZnS particle size. (b) Comparison of data using 0.1 mol L^{-1} (○) and 0.01 mol L^{-1} (□) $ZnCl_2$ solutions under a 10/30 H_2S/N_2 gas atmosphere and 1 mol L^{-1} $ZnCl_2$ solution under a pure H_2S atmosphere (◇). The lines have been added to indicate slightly different curve progressions.

in the jet have been calculated for short reaction times ($R_p = R_g(5/3)^{1/2}$, with R_g and R_p being the radii of gyration and of the particle). The calculated radii of gyration as obtained from the scattering curves measured at different reaction times are shown in Figure 3. The individual data points have been obtained from data sets which were collected during several measurement campaigns at Elettra, highlighting the high reproducibility of the measurements. Between individual campaigns were often time periods of several months, during which time the equipment had to be disassembled and removed from the beamline. Figure 3a shows data as obtained from 1 mol L^{-1} $ZnCl_2$ solutions under a dilute H_2S atmosphere (N_2/H_2S = 30 mL/10 mL). The two lines indicate two different growth scenarios. The solid line is the least-squares fit through all data points, assuming a linear volume growth of the particles, as would be typical for a reaction limited growth process with a $t^{1/3}$ (t = time) dependence of R_g. The dashed line is the fit through all data points for a $t^{1/2}$ dependent change of R_g, as could be expected for a diffusion-limited growth process. Due to the given data scatter, it is difficult to judge which curve is more representative of the measured data. However, within the limits of the time resolution, the intercept of both curves is so close to t = 0 s, that no indication of an induction time is apparent. This suggests instantaneous particle formation under the given reaction conditions. Assuming a linear volume growth (solid line), the growth rate of the particles (aggregates) under the given conditions can be calculated as about 4600 nm^3 μs^{-1}. This extremely rapid formation of rather large particles is a very surprising finding, and we first made sure that this was not due to artifacts brought about by the background correction or the data analysis routine. When NaCl solution was injected into a pure H_2S atmosphere as a control experiment, no scattering by particles was observed.

After having ascertained that the data are real, the question arises how they should be interpreted. From independent experiments on ZnS formation from Zn^{2+}- and S^{2-}-containing solutions analyzed in a stopped flow cell with UV/vis spectroscopy, it is known that individual ZnS particles have a size of approximately 1.5−2 nm after much longer reaction times (milliseconds).[6] However, UV/vis spectroscopy and SAXS probe different properties. While UV/vis spectroscopy analyzes domain sizes of primary particles, SAXS probes electron density differences: i.e., it would rather see aggregates (secondary particles) than individual primary particles. Thus, even on the 10 μs time scale, particles already grow by aggregation, and individual particles are formed even faster. This is corroborated by the light scattering analysis of solutions prepared in a manner identical with that for the stopped-flow UV/vis measurements. After longer reaction times aggregates with sizes from 50 to 100 nm are detected. It has been shown that ripening by coalescence seems to play a major role in ZnS particle growth under precipitation conditions. Our finding that substantial aggregation takes place at the earliest stages of particle formation[8] is consistent with the coalescence scenario.

Formation of ZnS under the conditions of the study is thus extremely rapid, so that one can speculate that the rate is basically governed by the uptake rate of sulfide into the liquid jet, with sulfide being the limiting reagent. As can be seen from Figure 3a, also this scenario would fit the existing data to certain extent. Calculating the number of H_2S molecules arriving at the surface of the jet, on the basis of the laminar boundary layer

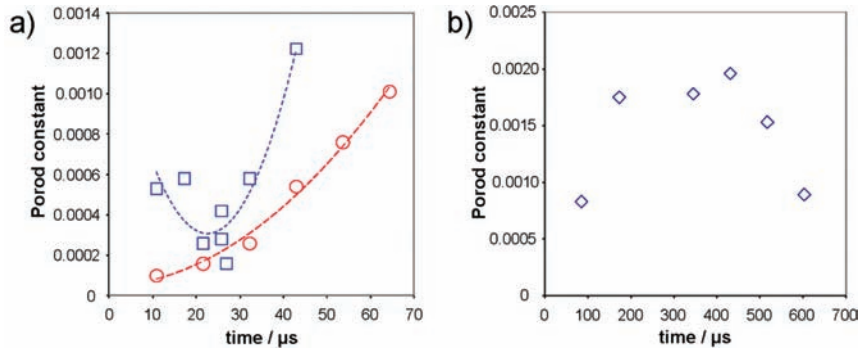

Figure 4. Porod constants from SAXS data measured on 1 mol L^{-1} $ZnCl_2$ solutions (a) at short reaction times under 10/30 H_2S/N_2 (squares) and pure H_2S atmospheres (circles) (the lines represent fits through the data sets) and (b) at longer reaction times under a 10/30 H_2S/N_2 atmosphere.

thickness after Boucher and Alves,[19] one can estimate that sufficient sulfide is present within a volume close to the surface of the liquid jet to allow formation of the observed particles. The size of this volume is determined by the diffusivity of the sulfide: i.e., the mean displacement within the reaction time (see the Supporting Information). As a consequence, particle formation and growth at ultrashort reaction times takes place only in a very thin top layer of a few hundred nanometers within the liquid jet. Under the chosen reaction conditions, the Zn^{2+} concentration appears to be sufficiently high to completely consume the incoming sulfide. The concentration of Zn^{2+} in the 1 mol L^{-1} solution is about 2 magnitudes higher than required for complete consumption of the absorbed sulfide. This conclusion is supported by concentration-dependent experiments, as shown in Figure 3b. The radii of gyration as measured for 0.01 mol L^{-1} $ZnCl_2$ solution deviate slightly from those measured for 1 mol L^{-1} solution. At somewhat longer reaction times, particle growth appears be slowed down for the 0.01 mol L^{-1} $ZnCl_2$ solution. A certain scatter of data points obviously exists. However, it appears that 1 mol L^{-1} $ZnCl_2$ solution contains sufficient amounts of Zn^{2+} to allow complete consumption of the sulfide input. The rate-limiting step for the 1 mol L^{-1} $ZnCl_2$ solution thus seems to be the diffusion of the H_2S into the liquid jet. Measurements under a pure H_2S atmosphere support this conclusion. They showed that substantially larger particles ($R_g > 50$ nm) were formed already after about 10 μs, as also shown in Figure 3b. The measurements under a pure hydrogen sulfide atmosphere caused frequent clogging of the nozzle, which also demonstrates the rapid formation of particles at very short reaction times. The input of hydrogen sulfide into the liquid jet thus appears to be the factor which mainly determines the growth rate of the particles.

For longer reaction times, scattering curves cannot be analyzed in the Guinier region any longer and particle sizes are not accessible directly form the scattering curve. However, the Porod region can be analyzed, from which the Porod constant, P, can be determined from the scattering intensities, I, and the scattering vectors, q, according to

$$I = \text{const} + \frac{P}{q^4}$$

The Porod constant for spherical particles is related to the particle radius R_p by

$$P \propto \frac{p\Delta\rho^2}{R_p}$$

with volume fraction of particles p, difference of electron density $\Delta\rho$, and the particle radius R_p.

As illustrated in Figure 4, the Porod constant increases at the early stages of particle formation, then passes a maximum, and finally decreases with prolonged reaction time. From the data in the Guinier range we know that the particles grow rapidly at ultrashort reaction times and then their sizes remain more or less constant. During the particle growth period at short reaction times the value of the Porod constant may even decrease slightly and pass through a minimum if the particle radii increase faster than the volume fraction (Figure 4a). A more rapid particle growth, as observed for experiments under a pure H_2S atmosphere, results in smaller Porod constants due to larger average particle sizes at a given residence time. With further progress of the reaction, the particle growth slows down and the sizes of the particles change at a much smaller rate. At the same time, the volume fraction of particles increases substantially, resulting in an increase of the Porod constant, as shown in parts a and b of Figure 4. In the range up to 200 μs, the volume fraction of the particles increases substantially while the sizes of the ZnS particles remain more or less constant, resulting in an increase of the Porod constants, as shown in Figure 4b. Finally, aggregation of those ZnS particles results in largely extended units with substantially higher radii. As a consequence, the Porod constant decreases, as observed for reaction times of more than 400 μs (Figure 4b). In the intermediate range, both effects cancel each other out and the progress of the Porod constant passes through a maximum. The development of the Porod constant is thus typical for particle aggregation.

Combining the results of previous investigations[6] and the above data, the ZnS particle formation proceeds as follows. Tiny primary ZnS particles with sizes of 1−2 nm form immediately when the H_2S enters the liquid jet. These particles tend to agglomerate to form aggregates with sizes in the range of 30−60 nm. These secondary particles (aggregates) have been observed in the SAXS experiments at residence times below 80 μs, and their final size strongly depends on the H_2S concentration of the gas atmosphere. With the progress of the reaction, these extended particles again accrete to form large extended aggregates, resulting in a decrease of the observed Porod constant at reaction times of some hundred microseconds. The particle formation of ZnS in precipitation reactions is thus strongly governed by aggregation processes. The reaction rate limiting

(19) Boucher, D. F.; Alves, G. E. In *Chemical Engineers' Handbook*, 5th ed.; Perry, R. H., Chilton, C. H., Eds.; McGraw-Hill: New York, 1973; pp 5-55−5-58.

process is the diffusion of the hydrogen sulfide from the gas phase into the liquid jet.

Conclusions

In summary, we have demonstrated the use of a novel continuous reactor which allows accessing extremely short reaction times in precipitation reactions, provided that one of the reagents can be introduced via the gas phase. This system has been used to study the formation of ZnS particles. Surprisingly, it was found that the ZnS particle formation is extremely rapid, with primary particles already formed at times lower than 10 μs without an apparent induction period. Growth of particles is then basically mass transfer limited. All sulfide species reaching the liquid jet surface are immediately consumed by the growing particles, the size of which is determined by the amount of material which can be collected by diffusion during the reaction time.

From the changes of the particle sizes with time in the early stages of the precipitation reaction and the change of the value of the Porod constant at somewhat longer reaction time, a conclusive picture could be drawn about the formation process of ZnS particles under the given experimental conditions. The process is strongly dominated by aggregation processes, and its reaction rate is controlled by the diffusion of hydrogen sulfide into the liquid phase.

Acknowledgment. We thank H. W. Schmidt (MPI Mülheim) for constructing the flow jet cell as well as N. Dufau (MPI Mülheim), J. Andersson (Abo Akademi), and Ö. Weiss (MPI Mülheim) for their support during measurement campaigns at Elettra. Partial financial support was obtained from the EU within the NUCLEUS project.

Supporting Information Available: Figures and text giving (1) details on the experimental setup, (2) a scheme of the tubular reactor concept, (3) calculations with respect to laminar/turbulent flow around the liquid jet, (4) an estimation of the thickness of the boundary layer around the liquid jet, an d(5) calculations with respect to diffusion of hydrogen sulfide into the liquid jet. This material is available free of charge via the Internet at http://pubs.acs.org.

JA101519Z